Journal of Zhejiang University-SCIENCE B (Biomedicine & Biotechnology) *2024 25(9):756-772*
www.jzus.zju.edu.cn; www.springer.com/journal/11585
E-mail: jzus_b@zju.edu.cn

Research Article
https://doi.org/10.1631/jzus.B2300691

Cynaroside regulates the AMPK/SIRT3/Nrf2 pathway to inhibit doxorubicin-induced cardiomyocyte pyroptosis

Hai ZOU[1,2], Mengyu ZHANG[3], Xue YANG[4], Huafeng SHOU[5], Zhenglin CHEN[6], Quanfeng ZHU[6], Ting LUO[7], Xiaozhou MOU[4,8]✉, Xiaoyi CHEN[4,8]✉

[1]*Department of Critical Care Medicine, Fudan University Shanghai Cancer Center, Shanghai 200032, China*
[2]*Department of Oncology, Shanghai Medical College, Fudan University, Shanghai 200032, China*
[3]*Xianghu Laboratory, Hangzhou 311231, China*
[4]*Clinical Research Institute, Key Laboratory of Tumor Molecular Diagnosis and Individualized Medicine of Zhejiang Province, Zhejiang Provincial People's Hospital (Affiliated People's Hospital), Hangzhou Medical College, Hangzhou 310014, China*
[5]*Center for Reproductive Medicine, Department of Gynecology, Zhejiang Provincial People's Hospital (Affiliated People's Hospital), Hangzhou Medical College, Hangzhou 310014, China*
[6]*Graduate School of Zhejiang Chinese Medical University, Hangzhou 310053, China*
[7]*State Key Laboratory for Managing Biotic and Chemical Threats to the Quality and Safety of Agro-products, Laboratory (Hangzhou) for Risk Assessment of Agricultural Products of Ministry of Agriculture, Institute of Agro-product Safety and Nutrition, Zhejiang Academy of Agricultural Sciences, Hangzhou 310021, China*
[8]*General Surgery, Cancer Center, Department of Hepatobiliary & Pancreatic Surgery and Minimally Invasive Surgery, Zhejiang Provincial People's Hospital (Affiliated People's Hospital), Hangzhou Medical College, Hangzhou 310014, China*

Abstract: Doxorubicin (DOX) is a commonly administered chemotherapy drug for treating hematological malignancies and solid tumors; however, its clinical application is limited by significant cardiotoxicity. Cynaroside (Cyn) is a flavonoid glycoside distributed in honeysuckle, with confirmed potential biological functions in regulating inflammation, pyroptosis, and oxidative stress. Herein, the effects of Cyn were evaluated in a DOX-induced cardiotoxicity (DIC) mouse model, which was established by intraperitoneal injections of DOX (5 mg/kg) once a week for three weeks. The mice in the treatment group received dexrazoxane, MCC950, and Cyn every two days. Blood biochemistry, histopathology, immunohistochemistry, reverse transcription-quantitative polymerase chain reaction (RT-qPCR), and western blotting were conducted to investigate the cardioprotective effects and potential mechanisms of Cyn treatment. The results demonstrated the significant benefits of Cyn treatment in mitigating DIC; it could effectively alleviate oxidative stress to a certain extent, maintain the equilibrium of cell apoptosis, and enhance the cardiac function of mice. These effects were realized via regulating the transcription levels of pyroptosis-related genes, such as nucleotide-binding oligomerization domain-like receptor protein 3 (*NLRP3*), *caspase-1*, and gasdermin D (*GSDMD*). Mechanistically, for DOX-induced myocardial injury, Cyn could significantly modulate the expression of pivotal genes, including adenosine monophosphate-activated protein kinase (*AMPK*), peroxisome proliferator-activated receptor γ coactivator-1α (*PGC-1α*), sirtuin 3 (*SIRT3*), and nuclear factor erythroid 2-related factor 2 (*Nrf2*). We attribute it to the mediation of AMPK/SIRT3/Nrf2 pathway, which plays a central role in preventing DOX-induced cardiomyocyte injury. In conclusion, the present study confirms the therapeutic potential of Cyn in DIC by regulating the AMPK/SIRT3/Nrf2 pathway.

Key words: Cynaroside; Doxorubicin; Pyroptosis; Cardiotoxicity; Oxidative stress

1 Introduction

Doxorubicin (DOX), an anthracycline drug sold under different brand names such as adriamycin, is widely used to treat hematological malignancies and various solid tumors (Stamm et al., 2021). While DOX has demonstrated clinical efficacy in this regard, including treatment for lymphoma, breast cancer, esophageal cancer, and osteosarcoma, its clinical

✉ Xiaozhou MOU, mouxz@zju.edu.cn
Xiaoyi CHEN, joicecxy@hotmail.com
Xiaozhou MOU, https://orcid.org/0000-0002-3234-1737
Xiaoyi CHEN, https://orcid.org/0000-0001-9160-7016
Hai ZOU, https://orcid.org/0000-0001-8580-4769

Received Oct. 6, 2023; Revision accepted Dec. 17, 2023;
Crosschecked Aug. 7, 2024; Published online Sept. 12, 2024

application has been associated with several significant side effects, most notably severe cardiotoxicity and heart failure, limiting its widespread use. The prevalence and incidence of DOX-induced cardiotoxicity (DIC) are of significant concern in the fields of oncology and cardiology: studies have reported DIC incidence rates ranging from 5% to 48%, with higher rates observed in patients receiving high cumulative doses or those with pre-existing cardiovascular risk factors (Meng et al., 2019; Wang et al., 2020; Rawat et al., 2021). Dexrazoxane (Dex) is the only US Food and Drug Administration (FDA)-approved cardioprotective agent with iron-chelating activity for treating DIC; however, its application is limited due to its potential for inducing secondary malignancies and aggravating myelosuppression (Macedo et al., 2019; Filomena et al., 2020; Yu et al., 2020). Consequently, there is an urgent need to develop novel therapeutic strategies and drugs to reduce the side effects of DOX and improve the overall efficacy of chemotherapeutic agents.

Pyroptosis is a recently recognized form of programmed cell death characterized by cell expansion, leading to cell membrane rupture and the release of cellular contents, including pro-inflammatory factors (Yu et al., 2021; Xiong et al., 2022; Chen et al., 2023). This process triggers a robust inflammatory response in surrounding tissues. Pyroptosis has been shown to play a pivotal role in the development of cardiovascular diseases, with recent studies implicating its involvement in the pathogenesis of DIC (Meng et al., 2019; Zeng et al., 2019; Zhang L et al., 2021). At present, considerable evidence points to a close association between abnormal activation of the nucleotide-binding oligomerization domain-like receptor protein 3 (NLRP3) inflammasome and cell pyroptosis. Specifically, the activation of NLRP3 inflammasome can initiate intracellular inflammatory reactions, ultimately leading to cell pyroptosis (Chen et al., 2023). Consequently, numerous studies have focused on inhibiting the activation of NLRP3, with particular attention to MCC950, a specific inhibitor of NLRP3. MCC950 intervenes in the activation process of the NLRP3 inflammasome, reducing or inhibiting the release of pro-inflammatory factors. This is accomplished by interacting with proteins within the NLRP3 inflammasome, preventing or attenuating their activation, thereby inhibiting the functionality of the NLRP3 inflammasome (Coll et al., 2019). Notably, however, previous research has suggested that MCC950 may exhibit toxicity to the liver and kidneys, with potential function impairment effects (Mangan et al., 2018). This phenomenon has prompted a growing interest in identifying natural compounds that can modulate cell pyroptosis and may serve as therapeutic agents.

Cynaroside (Cyn), as a flavonoid glycoside, has been found in high concentrations in honeysuckle and possesses anti-inflammatory properties (Bouyahya et al., 2023). Cyn consists of a flavone aglycone (luteolin) with a sugar moiety (glucose) attached to it. Studies have reported that Cyn can inhibit the production of pro-inflammatory cytokines, such as interleukin-1β (IL-1β) and tumor necrosis factor-α (TNF-α), in lipopolysaccharide (LPS)-induced macrophages (Pei et al., 2021). Furthermore, Cyn has been shown to mitigate oxidative stress and apoptosis in various cell types. The above findings suggest that Cyn has potential therapeutic benefits due to its anti-inflammatory and antioxidative properties, making it a promising natural compound for further research and potential applications in various medical contexts (Sun et al., 2011; Feng JH et al., 2021).

Despite the promising anti-inflammatory effects of Cyn, its beneficial function and mechanisms of action in pyroptosis have yet to be elucidated. Pyroptosis is a complex process that involves the activation of several signaling pathways, including the NLRP3 inflammasome and the caspase-1-dependent pathway (Liang et al., 2020; Zeng, 2020). Future studies need to elucidate the potential of Cyn in modulating these pathways and its effects on pyroptosis; more research in this area is essential to understand the therapeutic potential of Cyn in addressing pyroptosis-related conditions.

The present study aimed to explore the potential protective effect of Cyn in a mouse model of DOX-induced cardiac dysfunction by measuring the typical parameters of critical processes associated with the development of DIC, involving oxidative stress, inflammation, cardiomyocyte apoptosis, and pyroptosis. In particular, we sought to establish whether Cyn inhibits NLRP3 inflammasome activation to regulate DOX-induced cardiomyocyte pyroptosis. Our findings provide new insights into the mechanisms underlying the cardioprotective effects of Cyn and propose novel strategies for addressing DIC.

2 Materials and methods

2.1 Chemicals

DOX (CAS: 25316-40-9), Dex (CAS: 24584-09-6), Cyn (CAS: 5373-11-5), and MCC950 (CAS: 256373-96-3) were purchased from Shanghai Yuanye Biotechnology Co., Ltd. (Shanghai, China).

2.2 Animals and treatments

C57BL/6 mice (seven weeks old, male, and weighing 19–21 g, 48 mice in total) were purchased from the China National Laboratory Animal Resource Center (Shanghai, China) and acclimated in the animal facilities for one week under the environmental conditions of 22–24 ℃, 50%–55% humidity, and a 12-h light/dark cycle. All mice were provided with sterile food and water ad libitum.

The mice were randomized into six groups (eight mice per group): (1) normal control group (NC), (2) DOX group (DOX), (3) Dex group (DRZ), (4) MCC950 group (MCC), (5) low-dose Cyn group (Cyn-L), and (6) high-dose Cyn group (Cyn-H). After a one-week adaptation period, the experimental design was optimized according to the relevant literature (Grover et al., 2023; Tan et al., 2023). All groups received intraperitoneal injections of DOX (5 mg/kg) once a week for three weeks at a cumulative dose (Cd.) of 15 mg/kg, except the NC group. One day after weekly DOX treatment, the following drugs were administered to the respective groups three times a week, one day apart: DRZ (Dex, 50 mg/(kg·d) intraperitoneally (i.p.), 450 mg/kg Cd.), MCC (MCC950, 10 mg/(kg·d) i.p., 90 mg/kg Cd.), Cyn-L (Cyn, 10 mg/(kg·d) i.p., 90 mg/kg Cd.), and Cyn-H (Cyn, 50 mg/(kg·d) i.p., 450 mg/kg Cd.), while the NC and DOX groups were supplemented with the same volume of saline (Fu et al., 2020; Yu et al., 2020; Pei et al., 2021). On the 22nd day of the experiment, the mice were weighed and sacrificed by isoflurane inhalation, and their blood and hearts were collected for further analysis.

2.3 Biochemical analysis

The serum levels of alanine aminotransferase (ALT; C009-2-1), aspartate aminotransferase (AST; C010-2-1), malondialdehyde (MDA; A003-1-2), lactate dehydrogenase (LDH; A020-2-2), reduced glutathione (GSH; A006-2-1), superoxide dismutase (SOD; A001-3-2), and catalase (CAT; A007-1-1) activity were determined using kits obtained from the Nanjing Jiancheng Institute of Biological Engineering (Nanjing, China) following the manufacturer's instructions.

The serum levels of creatine kinase-MB (CK-MB; ml037723), cardiac troponin T (cTnT; ml037292), IL-1β (ml098416), and IL-18 (CK-E20324) were measured using enzyme-linked immunosorbent assay (ELISA) kits purchased from Shanghai Enzyme Biotechnology Co., Ltd. (Shanghai, China) following the provided instructions.

2.4 Cardiac histological and immunohistochemical assessment

The heart samples were immersed in 0.04 g/mL (4%) paraformaldehyde and fixed overnight. After selection, the samples underwent dehydration in alcohol, cleaning in xylene, and immersion in paraffin. Tissue sections were then collected using a microtome and slides were prepared. Hematoxylin and eosin (H&E) staining and wheat germ agglutinin (WGA) staining were performed for light microscopy analysis. Image-Pro Plus 6.0 (Media Cybernetics, Bethesda, MD, USA) was utilized to assess cardiomyocyte size for semi-quantitative analysis of the WGA staining results.

The effects of NLRP3, B-cell lymphoma-2 (Bcl-2), and Bcl-2-associated X protein (Bax) were detected by immunohistochemistry using corresponding antibodies. The positive areas of cardiac staining were calculated by Image-Pro Plus 6.0.

2.5 Reverse transcription-quantitative polymerase chain reaction (RT-qPCR)

Total RNA was extracted from the hearts using the TRIzol reagent (Invitrogen, 15596-018, Thermo Fisher Scientific, Waltham, MA, USA) and assessed for quantity and purity using ultraviolet spectrophotometry at 260 and 280 nm. Complementary DNA (cDNA) was synthesized using the HiScript® II Q RT SuperMix for qPCR from Vazyme (Nanjing, China). Real-time PCR was performed on the Opticon 2 Real-Time PCR Detection System (Bio-Rad, Hercules, CA, USA) using the SYBR Green PCR Master Mix (Roche Diagnostics, Basel, Switzerland) and the primer information is listed in Table 1. The PCR conditions were as follows: pre-denaturation at 95 ℃ for 30 s, followed by 40 cycles of denaturation at 95 ℃ for 10 s and annealing at 60 ℃ for 30 s. After the reaction, the cycle

Table 1 Primer sequences used in reverse transcription-quantitative polymerase chain reaction (RT-qPCR)

Gene	GenBank accession number	Forward primer sequence (5'→3')	Reverse primer sequence (5'→3')
ANP	NM_008725	GCTTCCAGGCCATATTGGAG	GGGGGCATGACCTCATCTT
BNP	NM_008726	GAGGTCACTCCTATCCTCTGG	GCCATTTCCTCCGACTTTTCTC
Myh7	NM_080728	ACTGTCAACACTAAGAGGGTCA	TTGGATGATTTGATCTTCCAGGG
Tnnt2	NM_011619	CAGAGGAGGCCAACGTAGAAG	CTCCATCGGGGATCTTGGGT
Tnni1	NM_001112702	ATGCCGGAAGTTGAGAGGAAA	TCCGAGAGGTAACGCACCTT
Actc1	NM_009608	CTGGATTCTGGCGATGGTGTA	CGGACAATTTCACGTTCAGCA
Sod2	NM_013671	CAGACCTGCCTTACGACTATGG	CTCGGTGGCGTTGAGATTGTT
Cat	NM_009804	AGCGACCAGATGAAGCAGTG	TCCGCTCTCTGTCAAAGTGTG
Nqo-1	NM_008706	AGGATGGGAGGTACTCGAATC	AGGCGTCCTTCCTTATATGCTA
Gclc	NM_010295	GGGGTGACGAGGTGGAGTA	GTTGGGGTTTGTCCTCTCCC
Bcl-2	NM_177410	GTCGCTACCGTCGTGACTTC	CAGACATGCACCTACCCAGC
Bax	NM_007527	TGAAGACAGGGGCCTTTTTG	AATTCGCCGGAGACACTCG
Foxo3	NM_019740	CTGGGGGAACCTGTCCTATG	TCATTCTGAACGCGCATGAAG
Birc5	NM_009689	CTACCGAGAACGAGCCTGATT	AGCCTTCCAATTCCTTAAAGCAG
Trp53	NM_011640	CTCTCCCCCGCAAAAGAAAAA	CGGAACATCTCGAAGCGTTTA
NLRP3	NM_145827	ATTACCCGCCCGAGAAAGG	TCGCAGCAAAGATCCACACAG
ASC	NM_023258	CTTGTCAGGGGATGAACTCAAAA	GCCATACGACTCCAGATAGTAGC
GSDMD	NM_026960	CCATCGGCCTTTGAGAAAGTG	ACACATGAATAACGGGGTTTCC
NEK7	NM_021605	GCTGTCTGCTATATGAGATGGC	CCGAATAGTGATCTGACGGGAG
IL-18	NM_008360	GTGAACCCCAGACCAGACTG	CCTGGAACACGTTTCTGAAAGA
IL-1β	NM_008361	GCAACTGTTCCTGAACTCAACT	ATCTTTTGGGGTCCGTCAACT
Caspase-1	NM_009807	AATACAACCACTCGTACACGTC	AGCTCCAACCCTCGGAGAAA
Caspase-3	NM_009810	ATGGAGAACAACAAAACCTCAGT	TTGCTCCCATGTATGGTCTTTAC
LKB1	NM_011492	TTGGGCCTTTTCTCCGAGG	CAGGTCCCCCATCAGGTACT
AMPK	NM_001170555	AAAGAACCCTAGCCTGAAGAGG	ACCTTCCGAGATGAATGCTTTT
PRKAA1	NM_001013367	GTCAAAGCCGACCCAATGATA	CGTACACGCAAATAATAGGGGTT
PRKAA2	NM_178143	CAGGCCATAAAGTGGCAGTTA	AAAAGTCTGTCGGAGTGCTGA
PGC-1α	NM_008904	TATGGAGTGACATAGAGTGTGCT	CCACTTCAATCCACCCAGAAAG
SIRT3	NM_001127351	ATCCCGGACTTCAGATCCCC	CAACATGAAAAAGGGCTTGGG
Nrf2	NM_010902	TCTTGGAGTAAGTCGAGAAGTGT	GTTGAAACTGAGCGAAAAAGGC
HO-1	NM_010442	AAGCCGAGAATGCTGAGTTCA	GCCGTGTAGATATGGTACAAGGA
Gapdh	NM_008084	CATCACTGCCACCCAGAAGACTG	ATGCCAGTGAGCTTCCCGTTCAG

ANP: atrial natriuretic peptide; *BNP*: brain natriuretic peptide; *Myh7*: myosin heavy chain 7; *Tnnt2*: troponin T2; *Tnni1*: troponin I1; *Actc1*: α-actin-1; *Sod2*: superoxide dismutase 2; *Cat*: catalase; *Nqo-1*: NAD(P)H:quinone oxidoreductase 1; *Gclc*: glutamate-cysteine ligase catalytic subunit; *Bcl-2*: B-cell lymphoma-2; *Bax*: Bcl-2-associated X protein; *Foxo3*: forkhead box protein O3; *Birc5*: baculoviral IAP repeat-containing protein 5; *Trp53*: tumor suppressor p53; *NLRP3*: nucleotide-binding oligomerization domain-like receptor protein 3; *ASC*: apoptosis-associated speck-like protein-containing CARD; *GSDMD*: gasdermin D; *NEK7*: never in mitosis A-related kinase 7; *IL-18*: interleukin-18; *LKB1*: liver kinase B1; *AMPK*: adenosine monophosphate-activated protein kinase; *PRKAA1*: 5'-AMP-activated protein kinase catalytic subunit α-1; *PGC-1α*: peroxisome proliferator-activated receptor γ coactivator-1α; *SIRT3*: sirtuin 3; *Nrf2*: nuclear factor erythroid 2-related factor 2; *HO-1*: heme oxygenase-1; *Gapdh*: glyceraldehyde-3-phosphate dehydrogenase.

threshold (C_T) values were quantitatively analyzed by the $2^{-\Delta\Delta C_T}$ method. The messenger RNA (mRNA) expression levels were determined by calculating the fold changes versus the control group.

2.6 Western blot

Cardiac tissue samples were homogenized in RIPA lysis buffer (Wuhan Servicebio Technology Co., Ltd., Wuhan, China). The protein concentrations were determined using the bicinchoninic acid (BCA) protein assay kit (Boster Biological Technology Co., Ltd., Wuhan, China). Subsequently, proteins were separated by sodium dodecyl sulfate-polyacrylamide gel electrophoresis (SDS-PAGE) and then transferred to nitrocellulose membranes. To block the nitrocellulose membranes, 5% (0.05 g/mL) skimmed milk was used. Next, the membranes were incubated overnight at 4 °C with specific antibodies, including anti-NLRP3 rabbit polyclonal

antibody (pAb) (GB114320-100, 1:1000 (volume ratio, the same below)), anti-phospho-adenosine monophosphate-activated protein kinase (anti-p-AMPK) rabbit pAb (GB114323-100, 1:700), and β-actin rabbit pAb (GB11001-100, 1:2000) (Wuhan Servicebio Technology Co., Ltd.). Afterwards, horseradish peroxidase (HRP)-conjugated goat anti-rabbit immunoglobulin G (IgG) (GB23303, 1:3000; Wuhan Servicebio Technology Co., Ltd.) was added, followed by incubation for 1 h. Then, the membranes were washed three times using Tris-buffered saline with Tween-20 (TBST; Thermo Fisher Scientific) before exposure. The chemiluminescent signals were detected using ChemiDoc™ Touch (Bio-Rad), and the band intensities were quantified using ImageJ (National Institutes of Health, Bethesda, MD, USA).

2.7 Data analysis

All data were shown as mean±standard deviation (SD), and the significant differences between groups were analyzed using one-way analysis of variance (ANOVA) and Tukey's test (SPSS Statistics 19 software, IBM, Armonk, NY, USA). Differences of $P<0.05$ were considered statistically significant.

3 Results

3.1 Effects of Cyn on DOX-induced changes of heart weight and body weight

Based on our experimental observations, mice in the NC group displayed normal growth patterns, had a healthy appetite, and were characterized by a lustrous fur. In stark contrast, mice in the DOX group showed signs of impaired growth, were noticeably underweight and frail, displayed signs of depression, and had disheveled fur that was prone to shedding.

As illustrated in Fig. 1, the body weight of mice subjected to DOX treatment was significantly lower than that of the NC group, regardless of the specific treatment regimen ($P<0.05$). Furthermore, the heart weight of DOX-treated mice was also reduced.

3.2 Effect of Cyn on DOX-induced cardiac injury

In order to assess the impact of Cyn on DOX-induced cardiac injury, we conducted measurements of various serum markers in mice. As depicted in Fig. 2, the serum levels of ALT (Fig. 2a), AST (Fig. 2b), LDH (Fig. 2c), CK-MB (Fig. 2d), and cTnT (Fig. 2e) were significantly elevated after DOX treatment ($P<0.05$), indicating the presence of cardiac injury induced by DOX. Our findings clearly demonstrated that Cyn treatment substantially alleviated the pathological elevation in these indicators, except cTnT, in a dose-dependent manner.

The histopathological analysis of cardiac tissues revealed significant differences among the experimental groups (Fig. 2f). The myocardium of mice in the NC group exhibited normal myogenic fiber structure, well-organized cardiomyocyte arrays, and a healthy interstitium. Conversely, the heart sections from mice in the DOX-treated group displayed myogenic fiber degeneration and destruction, localized cytoplasmic lysis, vacuolar degeneration, structural blurring, and disorganization.

However, in the Cyn groups, an improvement in the aforementioned conditions was evident, along with a reduction in edema, compared with the DOX group.

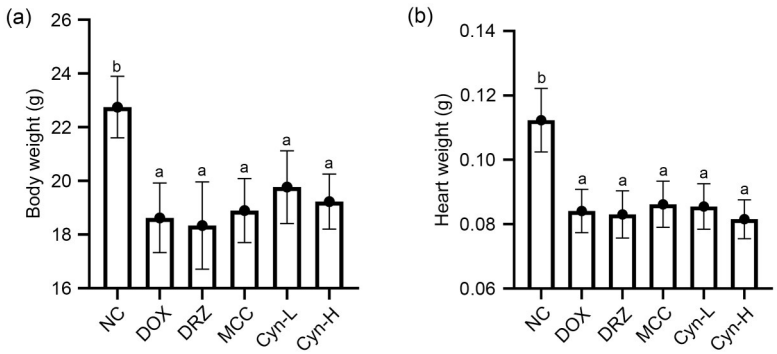

Fig. 1 Effects of cynaroside (Cyn) on doxorubicin (DOX)-induced weight changes. (a) Body weight; (b) Heart weight. Cyn administration alleviates DOX-induced body weight loss of mice. Data are represented as mean±standard deviation (SD), n=7 or 8. Different superscript letters indicate significant differences between groups ($P<0.05$). NC: normal control group; DOX: DOX group; DRZ: dexrazoxane group; MCC: MCC950 group; Cyn-L: low-dose Cyn group; Cyn-H: high-dose Cyn group.

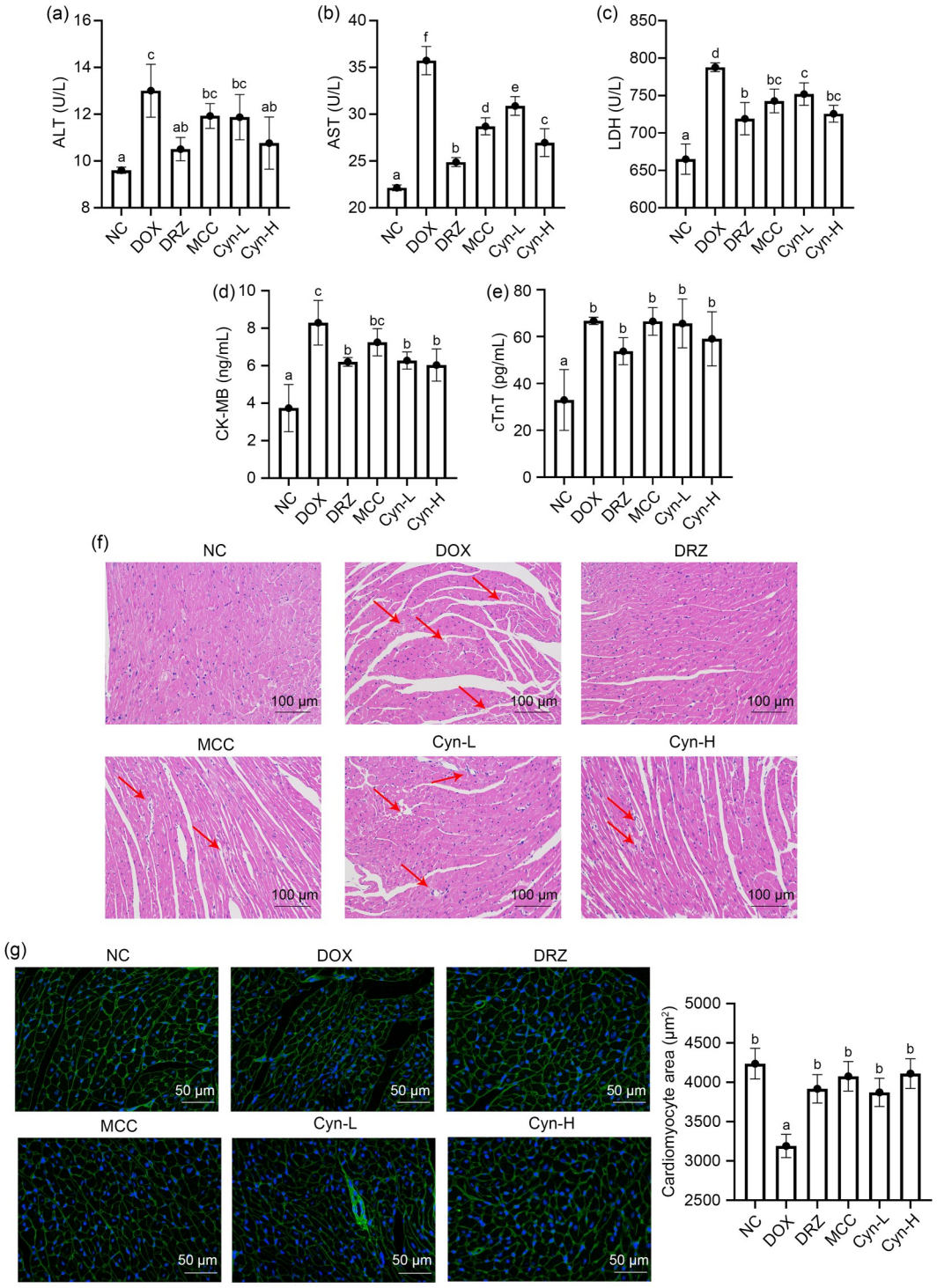

Fig. 2 Effect of cynaroside (Cyn) on doxorubicin (DOX)-induced cardiotoxicity (DIC). (a–e) Determination of serum alanine aminotransferase (ALT), aspartate aminotransferase (AST), lactate dehydrogenase (LDH), creatine kinase-MB (CK-MB), and cardiac troponin T (cTnT) levels in mice. (f) Histopathological examination of the heart by hematoxylin and eosin (H&E) staining. The lesion area is marked by a red arrow. (g) Histopathological examination of the heart by wheat germ agglutinin (WGA) staining and semi-quantitative cell size analysis. Data are represented as mean±standard deviation (SD), n=7 or 8. Different superscript letters indicate significant differences between groups (P<0.05). NC: normal control group; DOX: DOX group; DRZ: dexrazoxane group; MCC: MCC950 group; Cyn-L: low-dose Cyn group; Cyn-H: high-dose Cyn group.

In addition, WGA staining results (Fig. 2g) showed a significant reduction in the mean cross-sectional area of cardiomyocytes in the DOX group compared with the NC group (P<0.05). This, together with the results for heart weight, suggested that DOX administration caused cardiomyocyte atrophy in the mice, reducing their heart sizes.

Conversely, the mean cross-sectional areas of cardiomyocytes in the Cyn groups were significantly increased compared with the DOX group (P<0.05), indicating that Cyn effectively mitigated the cardiomyocyte atrophy induced by DOX administration. These results collectively support the potential cardioprotective effect of Cyn in counteracting DOX-induced cardiac injury.

3.3 Effect of Cyn on DOX-induced impairment of cardiac function

In order to further investigate the potential cardioprotective effect of Cyn against DOX-induced cardiac injury, we conducted measurements of the expression levels of several key genes associated with cardiac function and injury in mouse heart tissues. These genes included atrial natriuretic peptide (*ANP*) (Fig. 3a), brain natriuretic peptide (*BNP*) (Fig. 3b), myosin heavy chain 7 (*Myh7*) (Fig. 3c), troponin T2 (*Tnnt2*) (Fig. 3d), troponin I1 (*Tnni1*) (Fig. 3e), and α-actin-1 (*Actc1*) (Fig. 3f).

According to the results shown in Fig. 3, these genes exhibited upregulation in the DOX-treated group, indicating substantial cardiac injury. However, following treatment with Cyn, the abnormal expression of these genes was observed, in which the expression of several genes (e.g., *ANP*, *BNP*, and *Tnni1*) was notably reduced (P<0.05), suggesting that Cyn has the potential to alleviate the cardiac injury induced by DOX. The above results highlight the promising role of Cyn in both the prevention and treatment of DOX-induced cardiac injury.

3.4 Effect of Cyn on DOX-induced cardiac oxidative stress level

Oxidative damage is widely regarded as the primary cause of DIC. Thus, we examined the expression

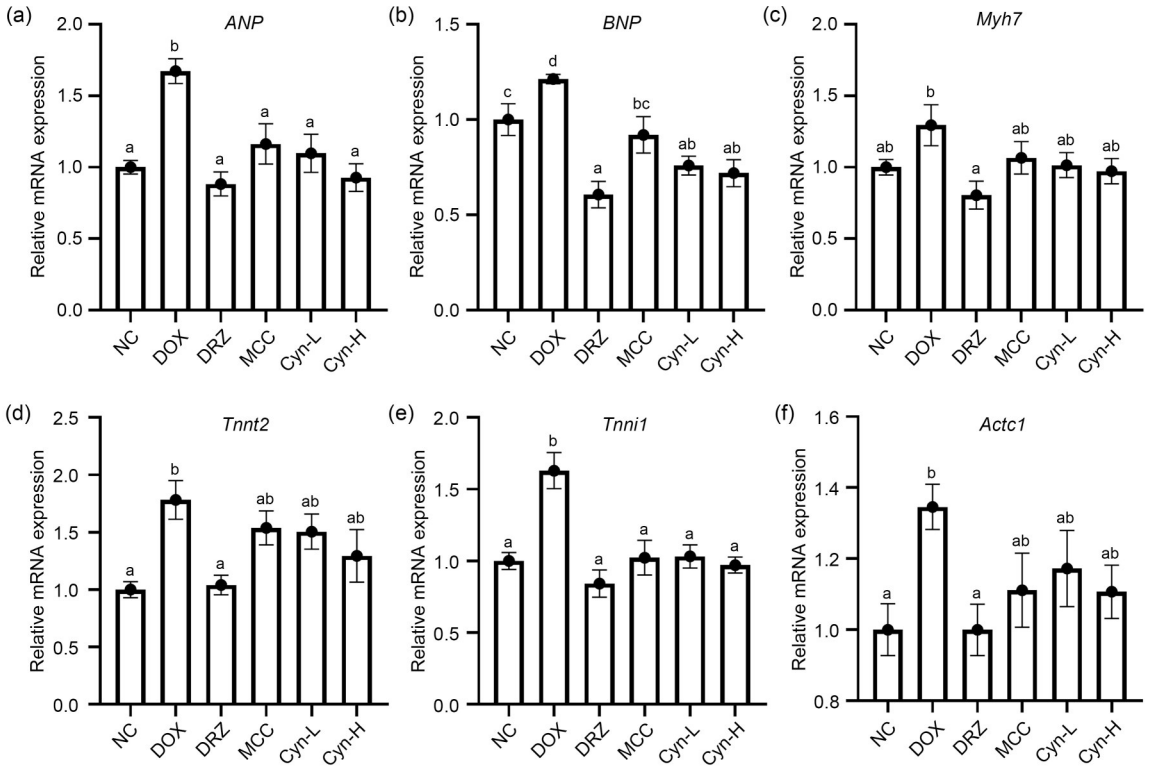

Fig. 3 Effect of cynaroside (Cyn) on doxorubicin (DOX)-induced impairment of cardiac function. The messenger RNA (mRNA) levels of atrial natriuretic peptide (*ANP*) (a), brain natriuretic peptide (*BNP*) (b), myosin heavy chain 7 (*Myh7*) (c), troponin T2 (*Tnnt2*) (d), troponin I1 (*Tnni1*) (e), and α-actin-1 (*Actc1*) (f) in cardiac tissue were determined by reverse transcription-quantitative polymerase chain reaction (RT-qPCR). Data are represented as mean±standard deviation (SD), n=7 or 8. Different superscript letters indicate significant differences between groups (P<0.05). NC: normal control group; DOX: DOX group; DRZ: dexrazoxane group; MCC: MCC950 group; Cyn-L: low-dose Cyn group; Cyn-H: high-dose Cyn group.

levels of oxidative stress-related markers in mouse heart tissues, as depicted in Fig. 4. Our findings indicated that DOX injection led to a significant increase in oxidative stress within the heart (P<0.05), as evidenced by elevated levels of MDA (Fig. 4d) and reduced levels of key antioxidant enzymes such as SOD (Fig. 4a), CAT (Fig. 4b), and GSH (Fig. 4c) in heart tissues.

However, compared with the DOX group, the cardiac tissues of mice treated with Cyn suppressed the abnormal expression of oxidative stress-related markers. Next, we delved into the expression levels of genes associated with oxidative stress. Our investigation revealed that DOX treatment resulted in a marked decrease in the mRNA expression of antioxidant enzymes in mice (P<0.05), including superoxide dismutase 2 (*Sod2*) (Fig. 4e), catalase (*Cat*) (Fig. 4f), NAD(P)H:quinone oxidoreductase 1 (*Nqo-1*) (Fig. 4g), and glutamate-cysteine ligase catalytic subunit (*Gclc*) (Fig. 4h). Conversely, the expression levels of *Sod2*, *Nqo-1*, and *Gclc* in the cardiac tissue cells after high-dose Cyn treatment were significantly upregulated (P<0.05). This provides compelling evidence on the ability of Cyn to effectively mitigate the oxidative stress-related damage inflicted by DOX on cardiac tissue cells.

The above findings strongly support the potential cardioprotective effects of Cyn against DOX-induced cardiac injury, mainly through its role in attenuating oxidative stress within the heart.

3.5 Effect of Cyn on DOX-induced apoptosis in cardiac cells

The primary pathological mechanism of DOX-induced cardiac injury lies in the excessive apoptosis of cardiomyocytes. To investigate the impact of Cyn on cardiomyocyte apoptosis, we conducted an immunohistochemical analysis, which revealed notable alterations in the expression of pro- and anti-apoptotic proteins. Specifically, in the DOX-treated group, the positive expression of the pro-apoptotic protein Bax indicated a significant increase, coupled with a significant decrease in the expression of the anti-apoptotic protein Bcl-2 (Figs. 5h and 5i; P<0.05).

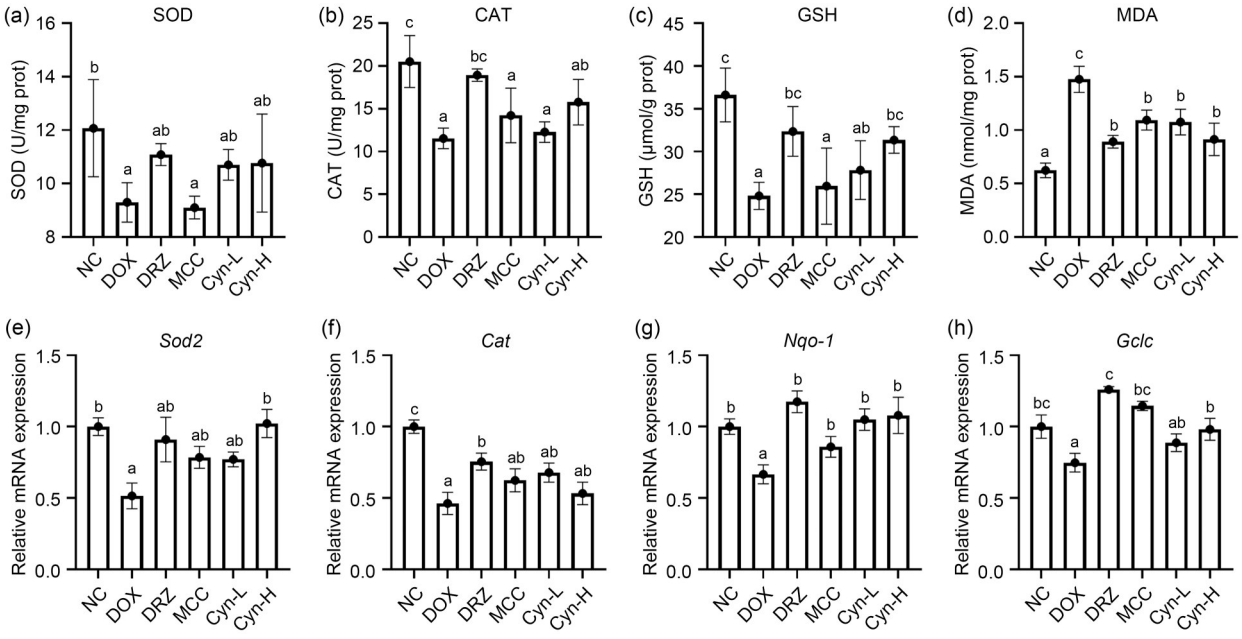

Fig. 4 Effect of cynaroside (Cyn) on doxorubicin (DOX)-induced cardiac oxidation levels. (a, b) The activity of antioxidant enzymes such as superoxide dismutase (SOD) and catalase (CAT). (c, d) The level of antioxidant reduced glutathione (GSH) and the peroxide indicator malondialdehyde (MDA). (e–h) The messenger RNA (mRNA) levels of superoxide dismutase 2 (*Sod2*), catalase (*Cat*), NAD(P)H: quinone oxidoreductase 1 (*Nqo-1*), and glutamate-cysteine ligase catalytic subunit (*Gclc*) in cardiac tissue determined by reverse transcription-quantitative polymerase chain reaction (RT-qPCR). Data are represented as mean±standard deviation (SD), n=7 or 8. Different superscript letters indicate significant differences between groups (P<0.05). NC: normal control group; DOX: DOX group; DRZ: dexrazoxane group; MCC: MCC950 group; Cyn-L: low-dose Cyn group; Cyn-H: high-dose Cyn group; prot: protein.

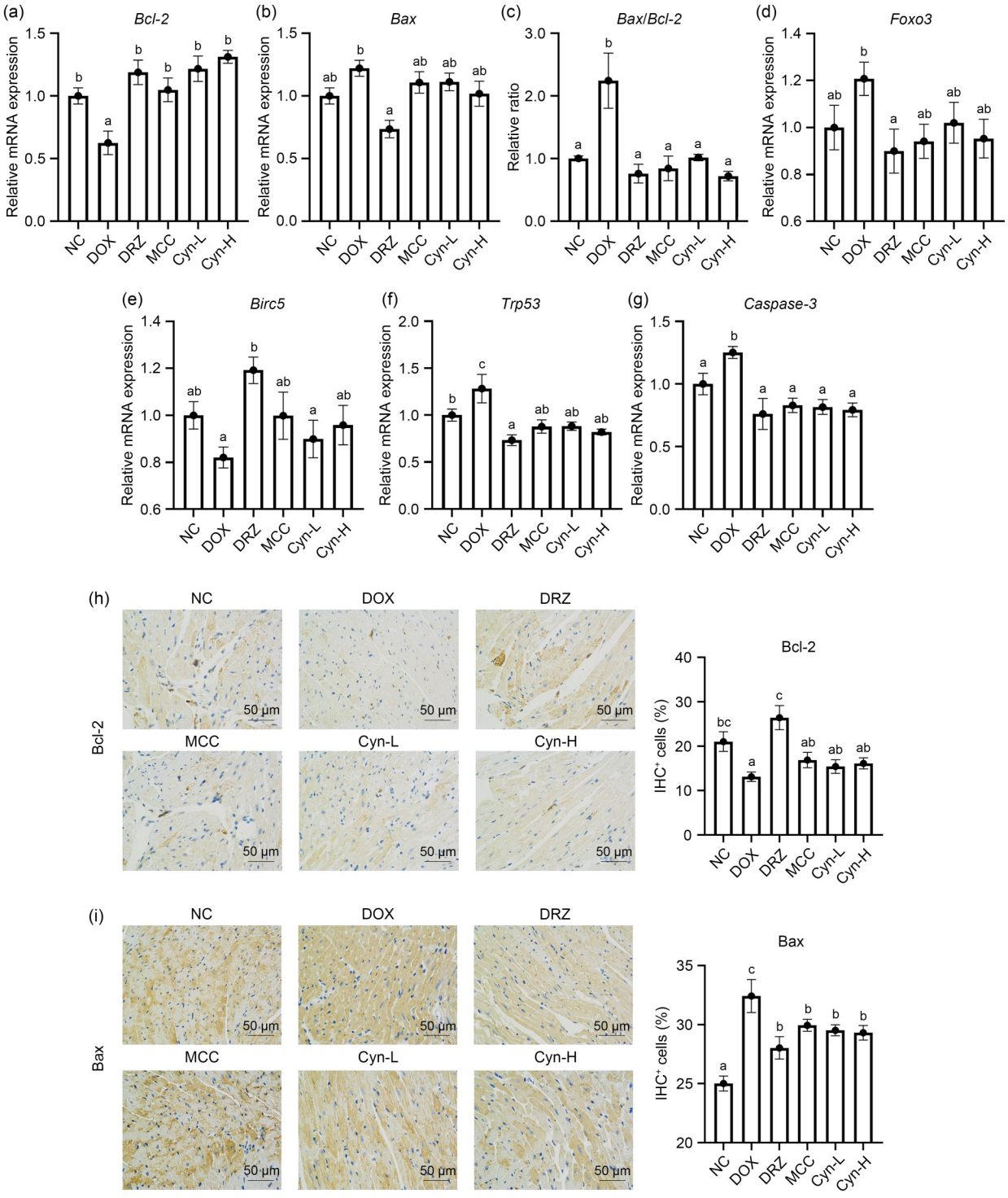

Fig. 5 Effect of cynaroside (Cyn) on doxorubicin (DOX)-induced apoptosis in cardiac cells. (a, b) The messenger RNA (mRNA) levels of B-cell lymphoma-2 (*Bcl-2*) and Bcl-2-associated X protein (*Bax*) in cardiac tissue were determined by reverse transcription-quantitative polymerase chain reaction (RT-qPCR). (c) The ratio of *Bax* to *Bcl-2* gene expression in mice. (d–g) The mRNA levels of forkhead box protein O3 (*Foxo3*), baculoviral IAP repeat-containing protein 5 (*Birc5*), tumor suppressor p53 (*Trp53*), and *caspase-3* in cardiac tissue were determined by RT-qPCR. (h, i) Results of immunohistochemical (IHC) analysis and quantification of Bcl-2 and Bax. Data are represented as mean±standard deviation (SD), n=7 or 8. Different superscript letters indicate significant differences between groups (P<0.05). NC: normal control group; DOX: DOX group; DRZ: dexrazoxane group; MCC: MCC950 group; Cyn-L: low-dose Cyn group; Cyn-H: high-dose Cyn group.

Next, we examined the expression of apoptosis-related genes within the cardiac tissues of mice from each group. The results demonstrated that the expression of *Bax* gene in cardiomyocytes was elevated after DOX treatment, signifying an upregulation of apoptotic activity. However, with the administration of Cyn, the expression level of *Bax* gene in mouse hearts decreased ($P>0.05$), whereas the expression level of *Bcl-2* gene increased ($P<0.05$). Consequently, the *Bax*/*Bcl-2* ratio exhibited significant downregulation ($P<0.05$), indicative of a shift towards a more anti-apoptotic state (Figs. 5a–5c). Similar trends were observed for other apoptosis-related genes: those associated with promoting apoptosis, such as forkhead box protein O3 (*Foxo3*) (Fig. 5d), tumor suppressor p53 (*Trp53*) (Fig. 5f), and *caspase-3* (Fig. 5g), displayed increased expression levels following DOX treatment, whereas the apoptosis-suppressing gene baculoviral IAP repeat-containing protein 5 (*Birc5*) (Fig. 5e) was suppressed. Remarkably, the administration of Cyn ameliorated these abnormal expression patterns, with *Trp53* and *Caspase-3* showing significant differences ($P<0.05$), suggesting that Cyn mitigated the aberrant apoptotic response to a certain extent. The above findings collectively indicate that Cyn has the potential to modulate the apoptotic response in cardiomyocytes, contributing to its role in alleviating DOX-induced cardiac injury.

3.6 Effect of Cyn on DOX-induced cardiac pyroptosis

A growing body of evidence has consistently signified the involvement of NLRP3-induced inflammatory responses and cellular pyroptosis in the pathophysiological process of DIC. In light of this, we conducted a comprehensive examination of the expression levels of cellular pyroptosis-related genes in mouse heart tissues, and the results are presented in Fig. 6. The immunohistochemical analysis revealed a significant increase in the activation of NLRP3, a pivotal player in triggering cellular pyroptosis, in the heart tissues of mice exposed to DOX (Fig. 6h). Subsequent assays further unveiled that the in vivo administration of DOX upregulated the mRNA levels of essential genes involved in cellular pyroptosis, including *NLRP3* (Fig. 6a), apoptosis-associated speck-like protein containing CARD (*ASC*) (Fig. 6b), gasdermin D (*GSDMD*) (Fig. 6c), never in mitosis A-related kinase 7 (*NEK7*) (Fig. 6d), *IL-18* (Fig. 6e), *IL-1β* (Fig. 6f), and *caspase-1* (Fig. 6g), all of which are crucial elements in the cellular pyroptosis process.

As a promising option, treatment with Cyn displayed a notable potential to mitigate the abnormal expression of the above genes. These findings strongly suggest that Cyn possesses the ability to serve as a therapeutic agent for inhibiting DOX-induced cardiomyocyte death caused by pyroptosis, which highlights Cyn as a potential candidate for preventing or treating DIC through its modulation of pyroptosis-related pathways.

3.7 Effect of Cyn on the AMPK/SIRT3/Nrf2 pathway

In order to gain further insights into the molecular mechanisms underlying the protective effect of Cyn against DOX-induced cardiac injury, we examined the expression levels of several key genes in mouse heart tissue, including liver kinase B1 (*LKB1*), *AMPK*, 5'-AMP-activated protein kinase catalytic subunit α-1 (*PRKAA1*), *PRKAA2*, peroxisome proliferator-activated receptor γ coactivator-1α (*PGC-1α*), sirtuin 3 (*SIRT3*), nuclear factor erythroid 2-related factor 2 (*Nrf2*), and heme oxygenase-1 (*HO-1*). The findings shown in Fig. 7 revealed that the model group exhibited decreased expression of these genes, suggesting that DOX induces oxidative stress and mitochondrial damage in cardiac tissue via inhibiting the AMPK/SIRT3/Nrf2 pathway.

Conversely, Cyn treatment was associated with increased expression of genes such as *LKB1*, *PGC-1α*, *SIRT3*, and *Nrf2*, indicating that Cyn can potentially mitigate oxidative stress and improve mitochondrial function by activating the AMPK/SIRT3/Nrf2 pathway. These observations provide valuable insights into the potential molecular mechanisms underlying the protective effects of Cyn against DOX-induced cardiac injury.

3.8 Effects of Cyn on p-AMPK and NLRP3 protein expression

In order to gain deeper insights into the mechanism of DOX-induced cardiac injury and the specific protective effects of Cyn, we conducted additional experiments to validate the involvement of two key factors previously identified in this process. By western blot analysis, we examined the expression levels of NLRP3 and p-AMPK proteins, and the results unveiled that DOX administration led to the aberrant expression of both proteins; however, treatment with Cyn

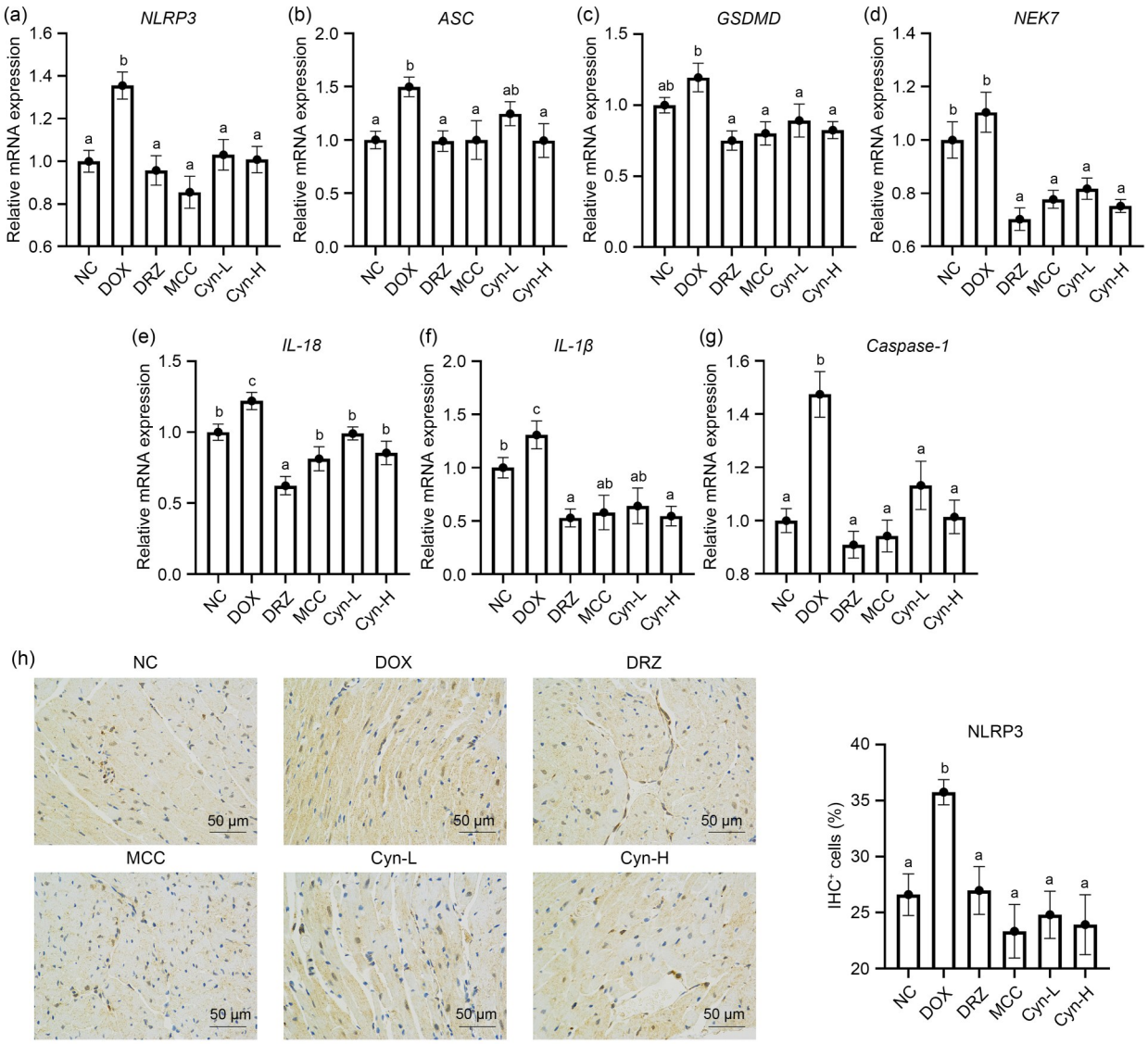

Fig. 6 Effect of cynaroside (Cyn) on doxorubicin (DOX)-induced pyroptosis. (a–g) The messenger RNA (mRNA) levels of nucleotide-binding oligomerization domain-like receptor protein 3 (*NLRP3*), apoptosis-associated speck-like protein containing CARD (*ASC*), gasdermin D (*GSDMD*), never in mitosis A-related kinase 7 (*NEK7*), interleukin-18 (*IL-18*), interleukin-1β (*IL-1β*), and *caspase-1* in cardiac tissue were determined by reverse transcription-quantitative polymerase chain reaction (RT-qPCR). (h) Results of immunohistochemical (IHC) analysis and quantification of NLRP3. Data are represented as mean±standard deviation (SD), *n*=7 or 8. Different superscript letters indicate significant differences between groups (*P*<0.05). NC: normal control group; DOX: DOX group; DRZ: dexrazoxane group; MCC: MCC950 group; Cyn-L: low-dose Cyn group; Cyn-H: high-dose Cyn group.

effectively regulated their expression, as depicted in Fig. 8 ($P<0.05$).

The above compelling results provide robust evidence supporting the beneficial role of Cyn in mitigating DOX-induced cardiac injury through the modulation of the AMPK/SIRT3/Nrf2 pathway and the involvement of NLRP3-mediated pyroptosis. These findings shed light on the mechanisms by which Cyn exerts its protective effects on DOX-induced cardiac injury, providing guidance in potential therapeutic interventions.

4 Discussion

DOX is a commonly used agent in anticancer therapy, while its associated cardiotoxicity remains a significant clinical challenge. Despite numerous

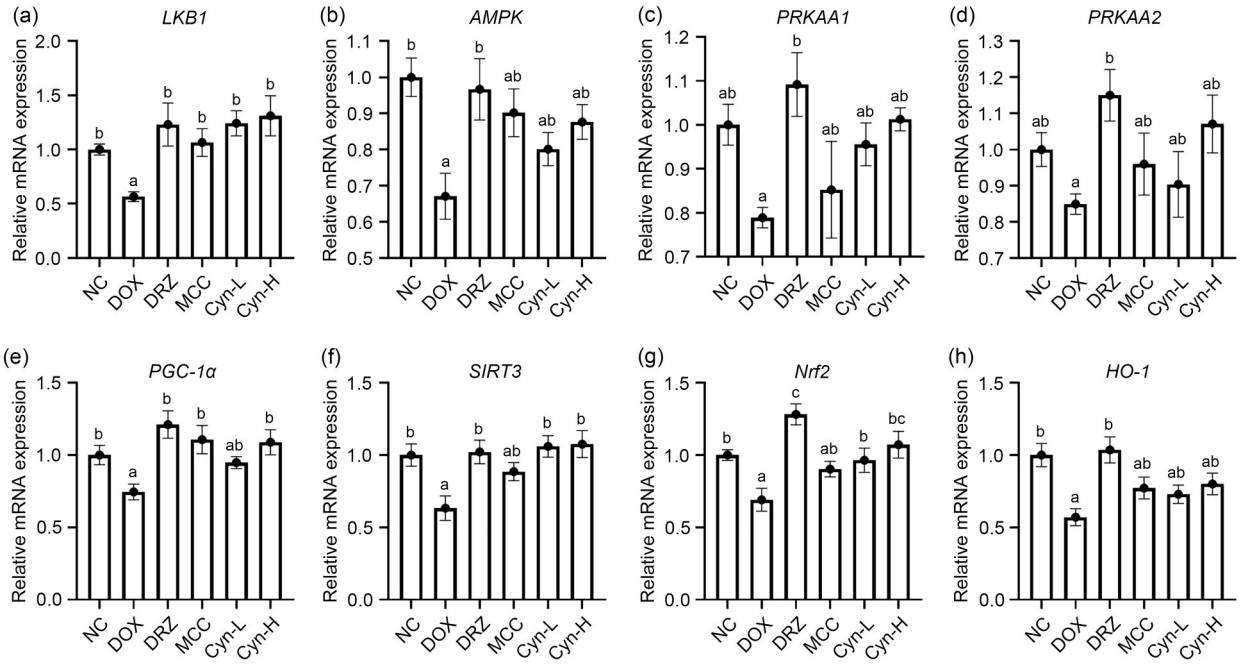

Fig. 7 Effect of cynaroside (Cyn) on the adenosine monophosphate-activated protein kinase (AMPK)/sirtuin 3 (SIRT3)/nuclear factor erythroid 2-related factor 2 (Nrf2) pathway. Transcript levels of liver kinase B1 (*LKB1*) (a), *AMPK* (b), 5'-AMP-activated protein kinase catalytic subunit α-1 (*PRKAA1*) (c), *PRKAA2* (d), peroxisome proliferator-activated receptor γ coactivator-1α (*PGC-1α*) (e), *SIRT3* (f), *Nrf2* (g), and heme oxygenase-1 (*HO-1*) (h) in cardiac tissue were determined by reverse transcription-quantitative polymerase chain reaction (RT-qPCR). Data are represented as mean± standard deviation (SD), *n*=7 or 8. Different superscript letters indicate significant differences between groups (*P*<0.05). NC: normal control group; DOX: DOX group; DRZ: dexrazoxane group; MCC: MCC950 group; Cyn-L: low-dose Cyn group; Cyn-H: high-dose Cyn group.

attempts to mitigate this issue, a pressing need remains to identify new targets and investigate potential therapeutic agents (Rawat et al., 2021; Yuan et al., 2023).

In our study, we administered Cyn to mice and observed substantial improvements in alleviating the adverse effects of DOX treatment. Cyn effectively mitigated weight loss and cardiac atrophy induced by DOX, as evidenced by the reduced serum LDH and CK-MB activity, indicating improved cardiac function. Furthermore, our experimental findings demonstrated that Cyn treatment attenuated DOX-induced oxidative stress and restored the balance of apoptotic mechanisms in cardiac tissue. Importantly, the data strongly suggested that Cyn is pivotal in alleviating DOX-induced NLRP3-mediated cardiomyocyte pyroptosis, and this protective effect is achieved through its regulatory effect on energy metabolism and the enhancement of the antioxidant capacity of cardiac cells. The underlying mechanism involves the activation of AMPK/SIRT3/Nrf2 pathway by Cyn, effectively countering the detrimental effects of DOX on cardiac cells. These remarkable findings provide a fresh perspective on addressing DIC and offer valuable support for developing novel therapeutic agents to tackle this important clinical concern. Our study demonstrated that, although Cyn showed positive effects on cardiac function and cell protection, no significant improvement was observed in body weight versus heart weight in mice. The possible explanations include factors such as treatment period and individual differences; however, this phenomenon deserves further study. Future work should further explore these factors to fully understand the potential effects of Cyn on body weight and heart weight, so as to help optimize treatment options and make them more consistent with the clinical application requirements.

Research has consistently demonstrated that DIC primarily operates through several interconnected pathways, including oxidative stress, inflammation, mitochondrial dysfunction, cardiomyocyte apoptosis, and excessive autophagy (Zhang YP et al., 2021; Liu and Zhao, 2022; Yin et al., 2022; Naderi et al., 2023). More recently, emerging evidence has highlighted a

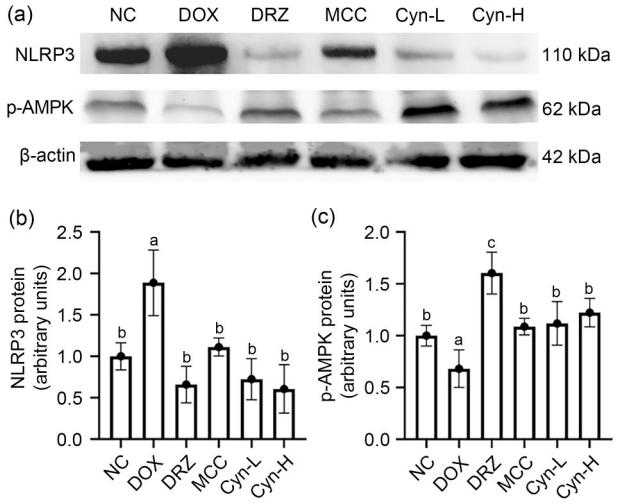

Fig. 8 Effects of cynaroside (Cyn) on doxorubicin (DOX)-induced expression of nucleotide-binding oligomerization domain-like receptor protein 3 (NLRP3) and adenosine monophosphate-activated protein kinase (AMPK) proteins in mouse cardiac tissue. (a) Representative western blot analyses of NLRP3 and phospho-AMPK (p-AMPK) proteins. (b, c) of Results densitometric analyses of NLRP3 and p-AMPK proteins. Data are represented as mean±standard deviation (SD), *n*=3. Different superscript letters indicate significant differences between groups (*P*<0.05). NC: normal control group; DOX: DOX group; DRZ: dexrazoxane group; MCC: MCC950 group; Cyn-L: low-dose Cyn group; Cyn-H: high-dose Cyn group.

novel form of inflammatory cell death known as pyroptosis, which also contributes to the pathogenesis of DIC (Gu et al., 2021). Specifically, in H9c2 cardiomyocytes, DOX-induced cell death has been linked to the Toll-like receptor 4 (TLR4)-NLRP3 inflammasome pathway, involving the secretion of inflammatory cytokines (Amin et al., 2023). The activation and assembly of NLRP3 ultimately trigger the activation of caspase-1, a pro-inflammatory cytokine, leading to the hydrolysis of pro-IL-1β into its active form, IL-1β. Furthermore, activated caspase-1 facilitates the cleavage of GSDMD, resulting in the formation of GSDMD-N terminus and its translocation, ultimately leading to the formation of membrane pores and the release of intracellular inflammatory cytokine IL-1β, culminating in cellular pyroptosis (Lin et al., 2020; Coll et al., 2022).

Experimental findings have unequivocally shown that Cyn treatment in mice effectively mitigates DOX-induced cardiac injury, an effect likely attributed to the activation of the AMPK/SIRT3/Nrf2 pathway by Cyn. Cyn modulates the energy metabolism of cardiac cells and enhances their antioxidant capacity through this pathway, alleviating DOX-induced NLRP3-mediated cardiomyocyte pyroptosis. These promising results suggest that Cyn holds significant potential as a therapeutic agent for addressing DIC. Simultaneously, we conducted comparative experiments to assess the impact of Dex and MCC950 on DOX-induced cardiac injury. The comparative results suggest that while Cyn may be slightly less effective than Dex in certain aspects, its performance is not significantly inferior to MCC950. This further underscores the considerable efficacy of Cyn in alleviating DOX-induced cardiac injury. Our observations provide valuable insights into future considerations for treating DIC, and suggest the potential for Cyn to serve as an alternative therapy in specific contexts.

Cyn as a flavonoid molecule possesses multiple biological activities, including antibacterial, anti-inflammatory, antioxidant, and antitumor properties (Yu HL et al., 2019; Lee et al., 2020; Bouyahya et al., 2023). Previous studies have reported that Cyn can promote anti-inflammatory M2 macrophage polarization, particularly in cases of multi-organ injury, by activating the Nrf2/HO-1 axis (Feng JF et al., 2021). In the context of this study, the regulation of the Nrf2/HO-1 axis by Cyn contributed to alleviating DOX-induced cardiac dysfunction, further supporting its cardioprotective effects.

Beyond the above effects, Cyn exhibits diverse actions in various biological contexts. For instance, Cyn has been observed to specifically target pyruvate kinase M2 (PKM2), inhibiting PKM2 nuclear translocation and the formation of the PKM2-hypoxia-inducible factor-1α (HIF-1α) complex. This results in the promotion of M1 to M2 macrophage conversion, effectively suppressing liver inflammation (Pei et al., 2021). Moreover, Cyn has shown promising effects in attenuating retinal damage induced by blue light irradiation, achieved by the inhibition of NLRP3 inflammasome activation and the subsequent reduction in inflammatory factor secretion (Feng JH et al., 2021). In line with these observations, the present study further indicates that Cyn effectively downregulates NLRP3 expression, thereby attenuating its impact on inflammatory cytokine secretion and cellular pyroptosis. However, the application of Cyn in the drug conversion process for flavonoids still faces some obstacles, such as issues related to bioavailability and toxicity, prompting further investigation in this field. Despite these challenges, research on other flavonoids such as quercetin has explored various drug delivery

systems to enhance their solubility and absorption, providing insights into the future application of Cyn and suggesting potential strategies to overcome its limitations (Sayed et al., 2019).

In the context of cellular metabolism, AMPK serves as a pivotal regulator with the capacity to suppress inflammation and oxidative stress. SIRT3, a member of the sirtuin family, primarily localizes within intracellular mitochondria, where it plays a crucial role in regulating apoptosis and autophagy in response to neuronal oxidative stress (Sun et al., 2018; Wu et al., 2019). Upon AMPK activation, the expression of PGC-1α is enhanced and SIRT3 becomes involved in the downstream regulation of PGC-1α, influencing metabolic processes (Wang DM et al., 2022; Wang ZR et al., 2022). Furthermore, the previous reseach demonstrated that SIRT3 overexpression and AMPK pathway activation in septic cardiomyopathy contribute to promoting biosynthesis within mitochondria, effectively ameliorating cardiomyocyte death (Guo et al., 2022).

The Nrf2/HO-1 signaling pathway plays a pivotal role in maintaining the body's antioxidant response by regulating the transcription, modification, or expression of downstream proteins, including HO-1, GSH, SOD, and fibroblast growth factor (FGF) (Xiao et al., 2021; Yao et al., 2023). Several studies have provided evidence that SIRT3 can activate Nrf2, and conversely, the Nrf2 system can suppress the expression of genes downstream of the NLRP3 inflammasome, resulting in reduced NLRP3 activation. Interestingly, NLRP3 activation can also influence the Nrf2 system (Chen et al., 2019; Bian et al., 2020; Zhang CY et al., 2021).

Based on our experimental findings, we propose the hypothesis that Cyn administration activates the expression of LKB1, which, in concert with AMPK, leads to the subsequent activation of PGC-1α and the release of SIRT3. Consequently, the expression of Nrf2 is enhanced, promoting elevated HO-1 expression and reducing the abnormal expression of NLRP3. Eventually, these orchestrated actions attenuate cellular scorching and alleviate cardiac injury.

Through the modulation of Nrf2/HO-1 signaling pathway, Cyn appears to choreograph a complex network of interactions involving LKB1, AMPK, PGC-1α, and SIRT3 to regulate cellular responses to oxidative stress and inflammation. By fine-tuning these key players, Cyn exerts protective effects against DIC and demonstrates potential as a therapeutic agent for countering oxidative damage and cellular pyroptosis in the context of cardiovascular diseases.

5 Conclusions

In conclusion, our study highlights the therapeutic potential of Cyn in mitigating DIC via the activation of AMPK/SIRT3/Nrf2 signaling pathway. By modulating cardiac cell energy metabolism and enhancing antioxidant capacity, Cyn shows significant potential in reducing DOX-induced oxidative stress, inflammatory cell death, and NLRP3-mediated cardiomyocyte pyroptosis. Given its versatile biological properties, encompassing anti-inflammatory, antioxidant, and antitumor effects, Cyn emerges as a compelling candidate for further investigation as a potential cardioprotective agent against DIC and other chemotherapy-related cardiac complications.

Despite the promising findings, our research has several limitations that must be considered. First, the study duration was relatively short, preventing a comprehensive assessment of the long-term effects of Cyn in therapeutic settings. Second, given our focus on using Cyn to treat DOX-induced cardiac injury, we have not delved into whether Cyn might impact cancer treatment or its specific effects on cancer patients. Future investigations should include an extended experimental period to validate our discoveries and further decipher the mechanisms by which Cyn operates within cancer cells, to assess its impact on cancer cell survival and proliferation. This will enable a thorough evaluation of the potential efficacy and safety of Cyn in cancer treatment. By addressing these issues, we aim to develop a more comprehensive understanding of the biological effects of Cyn, laying a solid foundation for the development of targeted and effective therapeutic strategies. Overall, our research contributes to expanding the knowledge base dedicated to enhancing the well-being and quality of life for cancer patients undergoing chemotherapy, promising a brighter future regarding the addressment of cardiac complications associated with cancer treatment.

Data availability statement

The data that support the findings of this study are available on request from the corresponding author. The data are not publicly available due to privacy or ethical restrictions.

Acknowledgments

This work was supported by the Zhejiang Traditional Chinese Medicine Science and Technology Project (Nos. 2022ZZ004 and GZY-ZJ-KJ-Z24062), China.

Author contributions

Hai ZOU and Mengyu ZHANG contributed equally to conceptualization, methodology, formal analysis, data curation, and writing – original draft. Xue YANG and Huafeng SHOU contributed to sample collection, data curation, and supervision. Zhenglin CHEN and Quanfeng ZHU contributed to data curation and visualization. Ting LUO contributed to investigation and writing – review & editing. Xiaozhou MOU and Xiaoyi CHEN contributed to funding acquisition and project administration. All authors have read and approved the final manuscript, and therefore, have full access to all the data in the study and take responsibility for the integrity and security of the data.

Compliance with ethics guidelines

Hai ZOU, Mengyu ZHANG, Xue YANG, Huafeng SHOU, Zhenglin CHEN, Quanfeng ZHU, Ting LUO, Xiaozhou MOU, and Xiaoyi CHEN declare that they have no conflict of interest.

All procedures followed were approved by the Animal Welfare and Research Ethics Committee of Zhejiang Provincial People's Hospital (No. 20230920152236938620). Every effort was made during the experiments to minimize animal suffering. All the institutional and national guidelines for the care and use of animals were followed.

References

Amin FM, Sharawy MH, Amin MN, et al., 2023. Nifuroxazide mitigates doxorubicin-induced cardiovascular injury: insight into oxidative/NLRP3/GSDMD-mediated pyroptotic signaling modulation. *Life Sci*, 314:121311. https://doi.org/10.1016/j.lfs.2022.121311

Bian HT, Wang GH, Huang JJ, et al., 2020. Dihydrolipoic acid protects against lipopolysaccharide-induced behavioral deficits and neuroinflammation via regulation of Nrf2/HO-1/NLRP3 signaling in rat. *J Neuroinflammation*, 17(1):166. https://doi.org/10.1186/s12974-020-01836-y

Bouyahya A, Taha D, Benali T, et al., 2023. Natural sources, biological effects, and pharmacological properties of cynaroside. *Biomed Pharmacother*, 161:114337. https://doi.org/10.1016/j.biopha.2023.114337

Chen Y, Liu YH, Jiang K, et al., 2023. Linear ubiquitination of LKB1 activates AMPK pathway to inhibit NLRP3 inflammasome response and reduce chondrocyte pyroptosis in osteoarthritis. *J Orthop Translat*, 39:1-11. https://doi.org/10.1016/j.jot.2022.11.002

Chen ZM, Zhong H, Wei JS, et al., 2019. Inhibition of Nrf2/HO-1 signaling leads to increased activation of the NLRP3 inflammasome in osteoarthritis. *Arthritis Res Ther*, 21:300. https://doi.org/10.1186/s13075-019-2085-6

Coll RC, Hill JR, Day CJ, et al., 2019. MCC950 directly targets the NLRP3 ATP-hydrolysis motif for inflammasome inhibition. *Nat Chem Biol*, 15(6):556-559. https://doi.org/10.1038/s41589-019-0277-7

Coll RC, Schroder K, Pelegrín P, 2022. NLRP3 and pyroptosis blockers for treating inflammatory diseases. *Trends Pharmacol Sci*, 43(8):653-668. https://doi.org/10.1016/j.tips.2022.04.003

Feng JF, Liu ZJ, Chen H, et al., 2021. Protective effect of cynaroside on sepsis-induced multiple organ injury through Nrf2/HO-1-dependent macrophage polarization. *Eur J Pharmacol*, 911:174522. https://doi.org/10.1016/j.ejphar.2021.174522

Feng JH, Dong XW, Yu HL, et al., 2021. Cynaroside protects the blue light-induced retinal degeneration through alleviating apoptosis and inducing autophagy *in vitro* and *in vivo*. *Phytomedicine*, 88:153604. https://doi.org/10.1016/j.phymed.2021.153604

Filomena D, Versacci P, Cimino S, et al., 2020. Echocardiographic long-term follow-up of adult survivors of pediatric cancer treated with Dexrazoxane-Anthracyclines association. *Int J Cardiol*, 299:271-275. https://doi.org/10.1016/j.ijcard.2019.07.096

Fu Q, Li J, Qiu LL, et al., 2020. Inhibiting NLRP3 inflammasome with MCC950 ameliorates perioperative neurocognitive disorders, suppressing neuroinflammation in the hippocampus in aged mice. *Int Immunopharmacol*, 82:106317. https://doi.org/10.1016/j.intimp.2020.106317

Grover SP, Bharathi V, Posma JJ, et al., 2023. Thrombin-mediated activation of PAR1 enhances doxorubicin-induced cardiac injury in mice. *Blood Adv*, 7(10):1945-1953. https://doi.org/10.1182/bloodadvances.2022008637

Gu JW, Huang H, Liu CL, et al., 2021. Pinocembrin inhibited cardiomyocyte pyroptosis against doxorubicin-induced cardiac dysfunction via regulating Nrf2/Sirt3 signaling pathway. *Int Immunopharmacol*, 95:107533. https://doi.org/10.1016/j.intimp.2021.107533

Guo Z, Tuo H, Tang N, et al., 2022. Neuraminidase 1 deficiency attenuates cardiac dysfunction, oxidative stress, fibrosis, inflammatory via AMPK-SIRT3 pathway in diabetic cardiomyopathy mice. *Int J Biol Sci*, 18(2):826-840. https://doi.org/10.7150/ijbs.65938

Lee SA, Park BR, Moon SM, et al., 2020. Cynaroside protects human periodontal ligament cells from lipopolysaccharide-induced damage and inflammation through suppression of NF-κB activation. *Arch Oral Biol*, 120:104944. https://doi.org/10.1016/j.archoralbio.2020.104944

Liang Q, Cai WY, Zhao YX, et al., 2020. Lycorine ameliorates bleomycin-induced pulmonary fibrosis via inhibiting NLRP3 inflammasome activation and pyroptosis. *Pharmacol Res*, 158:104884. https://doi.org/10.1016/j.phrs.2020.104884

Lin YQ, Luo TY, Weng AL, et al., 2020. Gallic acid alleviates gouty arthritis by inhibiting NLRP3 inflammasome activation and pyroptosis through enhancing Nrf2 signaling. *Front Immunol*, 11:580593.

https://doi.org/10.3389/fimmu.2020.580593

Liu DW, Zhao L, 2022. Spinacetin alleviates doxorubicin-induced cardiotoxicity by initiating protective autophagy through SIRT3/AMPK/mTOR pathways. *Phytomedicine*, 101: 154098.
https://doi.org/10.1016/j.phymed.2022.154098

Macedo AVS, Hajjar LA, Lyon AR, et al., 2019. Efficacy of dexrazoxane in preventing anthracycline cardiotoxicity in breast cancer. *JACC CardioOncol*, 1(1):68-79.
https://doi.org/10.1016/j.jaccao.2019.08.003

Mangan MSJ, Olhava EJ, Roush WR, et al., 2018. Targeting the NLRP3 inflammasome in inflammatory diseases. *Nat Rev Drug Discov*, 17(8):588-606.
https://doi.org/10.1038/nrd.2018.97

Meng LP, Lin H, Zhang J, et al., 2019. Doxorubicin induces cardiomyocyte pyroptosis via the TINCR-mediated post-transcriptional stabilization of NLR family pyrin domain containing 3. *J Mol Cell Cardiol*, 136:15-26.
https://doi.org/10.1016/j.yjmcc.2019.08.009

Naderi Y, Khosraviani S, Nasiri S, et al., 2023. Cardioprotective effects of minocycline against doxorubicin-induced cardiotoxicity. *Biomed Pharmacother*, 158:114055.
https://doi.org/10.1016/j.biopha.2022.114055

Pei LH, Le YF, Chen H, et al., 2021. Cynaroside prevents macrophage polarization into pro-inflammatory phenotype and alleviates cecal ligation and puncture-induced liver injury by targeting PKM2/HIF-1α axis. *Fitoterapia*, 152:104922.
https://doi.org/10.1016/j.fitote.2021.104922

Rawat PS, Jaiswal A, Khurana A, et al., 2021. Doxorubicin-induced cardiotoxicity: an update on the molecular mechanism and novel therapeutic strategies for effective management. *Biomed Pharmacother*, 139:111708.
https://doi.org/10.1016/j.biopha.2021.111708

Sayed N, Khurana A, Godugu C, 2019. Pharmaceutical perspective on the translational hurdles of phytoconstituents and strategies to overcome. *J Drug Deliv Sci Technol*, 53: 101201.
https://doi.org/10.1016/j.jddst.2019.101201

Stamm P, Kirmes I, Palmer A, et al., 2021. Doxorubicin induces wide-spread transcriptional changes in the myocardium of hearts distinguishing between mice with preserved and impaired cardiac function. *Life Sci*, 284:119879.
https://doi.org/10.1016/j.lfs.2021.119879

Sun W, Liu CX, Chen QH, et al., 2018. SIRT3: a new regulator of cardiovascular diseases. *Oxid Med Cell Longev*, 2018:7293861.
https://doi.org/10.1155/2018/7293861

Sun X, Sun GB, Wang M, et al., 2011. Protective effects of cynaroside against H_2O_2-induced apoptosis in H9c2 cardiomyoblasts. *J Cell Biochem*, 112(8):2019-2029.
https://doi.org/10.1002/jcb.23121

Tan X, Zhang RY, Lan MD, et al., 2023. Integration of transcriptomics, metabolomics, and lipidomics reveals the mechanisms of doxorubicin-induced inflammatory responses and myocardial dysfunction in mice. *Biomed Pharmacother*, 162:114733.
https://doi.org/10.1016/j.biopha.2023.114733

Wang DM, Cao LY, Zhou X, et al., 2022. Mitigation of honokiol on fluoride-induced mitochondrial oxidative stress, mitochondrial dysfunction, and cognitive deficits through activating AMPK/PGC-1α/Sirt3. *J Hazard Mater*, 437: 129381.
https://doi.org/10.1016/j.jhazmat.2022.129381

Wang X, Gao YH, Tian YH, et al., 2020. Integrative serum metabolomics and network analysis on mechanisms exploration of Ling-Gui-Zhu-Gan Decoction on doxorubicin-induced heart failure mice. *J Ethnopharmacol*, 250: 112397.
https://doi.org/10.1016/j.jep.2019.112397

Wang ZR, Yao MR, Jiang LY, et al., 2022. Dexmedetomidine attenuates myocardial ischemia/reperfusion-induced ferroptosis via AMPK/GSK-3β/Nrf2 axis. *Biomed Pharmacother*, 154:113572.
https://doi.org/10.1016/j.biopha.2022.113572

Wu J, Zeng ZH, Zhang WJ, et al., 2019. Emerging role of SIRT3 in mitochondrial dysfunction and cardiovascular diseases. *Free Radic Res*, 53(2):139-149.
https://doi.org/10.1080/10715762.2018.1549732

Xiao L, Dai ZW, Tang WJ, et al., 2021. Astragaloside IV alleviates cerebral ischemia-reperfusion injury through NLRP3 inflammasome-mediated pyroptosis inhibition via activating Nrf2. *Oxid Med Cell Longev*, 2021:9925561.
https://doi.org/10.1155/2021/9925561

Xiong X, Lu LH, Wang ZY, et al., 2022. Irisin attenuates sepsis-induced cardiac dysfunction by attenuating inflammation-induced pyroptosis through a mitochondrial ubiquitin ligase-dependent mechanism. *Biomed Pharmacother*, 152: 113199.
https://doi.org/10.1016/j.biopha.2022.113199

Yao Y, Wang HH, Yang Y, et al., 2023. Dehydroepiandrosterone protects against oleic acid-triggered mitochondrial dysfunction to relieve oxidative stress and inflammation via activation of the AMPK-Nrf2 axis by targeting GPR30 in hepatocytes. *Mol Immunol*, 155:110-123.
https://doi.org/10.1016/j.molimm.2023.01.008

Yin YL, Niu QQ, Hou HY, et al., 2022. PAE ameliorates doxorubicin-induced cardiotoxicity via suppressing NHE1 phosphorylation and stimulating PI3K/AKT phosphorylation. *Int Immunopharmacol*, 113:109274.
https://doi.org/10.1016/j.intimp.2022.109274

Yu HL, Li JY, Hu XL, et al., 2019. Protective effects of cynaroside on oxidative stress in retinal pigment epithelial cells. *J Biochem Mol Toxicol*, 33(8):e22352.
https://doi.org/10.1002/jbt.22352

Yu P, Zhang X, Liu N, et al., 2021. Pyroptosis: mechanisms and diseases. *Signal Transduct Target Ther*, 6:128.
https://doi.org/10.1038/s41392-021-00507-5

Yu XX, Ruan Y, Huang XQ, et al., 2020. Dexrazoxane ameliorates doxorubicin-induced cardiotoxicity by inhibiting

both apoptosis and necroptosis in cardiomyocytes. *Biochem Biophys Res Commun*, 523(1):140-146. https://doi.org/10.1016/j.bbrc.2019.12.027

Yuan CY, Wu Z, Jin CL, et al., 2023. Qiangxin recipe improves doxorubicin-induced chronic heart failure by enhancing KLF5-mediated glucose metabolism. *Phytomedicine*, 112: 154697. https://doi.org/10.1016/j.phymed.2023.154697

Zeng C, 2020. NLRP3 inflammasomes-mediated pyroptosis contributes to dilated cardiomyopathy and doxorubicin-induced cardiotoxicity. *J Mol Cell Cardiol*, 140(Suppl):22. https://doi.org/10.1016/j.yjmcc.2019.11.050

Zeng ZL, Li GH, Wu SY, et al., 2019. Role of pyroptosis in cardiovascular disease. *Cell Prolif*, 52(2):e12563. https://doi.org/10.1111/cpr.12563

Zhang CY, Zhao M, Wang BW, et al., 2021. The Nrf2-NLRP3-caspase-1 axis mediates the neuroprotective effects of Celastrol in Parkinson's disease. *Redox Biol*, 47:102134. https://doi.org/10.1016/j.redox.2021.102134

Zhang L, Jiang YH, Fan CD, et al., 2021. MCC950 attenuates doxorubicin-induced myocardial injury *in vivo* and *in vitro* by inhibiting NLRP3-mediated pyroptosis. *Biomed Pharmacother*, 143:112133. https://doi.org/10.1016/j.biopha.2021.112133

Zhang YP, Ni L, Lin BW, et al., 2021. SNX17 protects the heart from doxorubicin-induced cardiotoxicity by modulating LMOD2 degradation. *Pharmacol Res*, 169:105642. https://doi.org/10.1016/j.phrs.2021.105642